ChemPubSoc Europe

DOI: 10.1002/chem.201806053

CHEMISTRY A European Journal Communication

Fullerenes

Site-selective Synthesis of β-[70]PCBM-like Fullerenes: Efficient Application in Perovskite Solar Cells

Sara Vidal,[a] Marta Izquierdo,[a] Salvatore Filippone,[a] Israel Fernández,[a] Seckin Akin,[b, c] Ji-Youn Seo,[b] Shaik M. Zakeeruddin,*[b] Michael Grätzel,*[b] and Nazario Martín*[a, d]

Dedicated to Professor Maurizio Prato on the occasion of his 65th birthday

Abstract: We report on the site-selective synthesis of PCBM-like [70]fullerene site-isomers, where the elusive β-site-isomers are, for the first time, the major product in a (cyclo)addition chemical reaction involving [70]fullerene. The reaction involves an straightforward cyclopropanation of [70]fullerene from sulfonium salts, affording a mixture of α and β site-isomers in good yields. Amazingly, the preference for the α- or β-site-isomer can be efficiently controlled by means of the solvent polarity! DFT theoretical calculations (DMF and toluene) nicely predict that, although the formation of the α-adduct is, as expected, thermodynamically favored, the selectivity of the process is determined by the energy difference of the respective transition states. Furthermore, the employ of α or/and β site-isomers, as pure materials or as a mixture of them, used as templating agent, has been evaluated in perovskite solar cells. The positive influence of the [70]fullerenes by passivating the voids/pin-holes and/or deep slits, is reflected in highly efficient and stable bulk heterojunction perovskite solar cells, whose performance (around 20%) is slightly but consistently depending on the isomeric fullerene composition. These experimental findings pave the way to investigate a new reactivity on C_{70} and to explore the properties of the less-known β-derivatives.

Fullerene derivatives, namely C_{60} and C_{70}, have been traditionally considered as the ideal components for organic solar cells due to their exceptional optoelectronic and chemical properties.[1,2] Actually, films of fullerene derivatives have shown to possess a good electronic mobility and, therefore, to be effective solution-processable organic n-type semiconductors in different organic electronic applications.[3,4] Interestingly, [70]fullerene derivatives are preferentially used as compared to their [60]fullerene counterparts, due to a significant increase in their absorption coefficients in the visible region.[5] However, the control of the isomeric purity (up to four site-isomers are possible due to the D_{5h} symmetry of the C_{70} cage) of the involved higher fullerene derivatives remains challenging.[6]

Despite various non-fullerene electron acceptors have been reported,[7] the fullerene derivative $PC_{71}BM$ ([6,6]-phenyl C_{71} butyric acid methyl ester) is still considered as the reference acceptor in photovoltaic systems because of its low reorganization energy and appropriate molecular orbital energy.[1b,2h]

In the last few years, the photovoltaic field has experienced an important breakthrough due to the development of perovskite solar cells (PSCs).[8] PSCs have reached a power conversion efficiency (PCE) up to 23.7%.[9] In inverted device architecture, perovskite layer is sandwiched in between an electron transporting layer (ETL),[10] typically a fullerene derivative, and a hole transporting layer (HTL).[11] In regular device architectures, fullerene derivatives can be easily integrated into the PSCs as template to control the nucleation and crystal growth, resulting in a considerable increase in both the overall efficiency and long-term stability. However, in addition to the chemical composition of the fullerene derivative, the isomeric purity also plays a significant role for the structural control and final performance of the photovoltaic cells.

In particular, the isomeric effects of fullerene-based electron acceptors have led to some contradictions on isomer-dependent photovoltaic performance.[12] Recently, Grätzel et al. reported the use of pure bis-[60]PCBM in PSCs leading to higher photovoltaic performance.[10d] The use of pure isomers for improving the performance of the device has been demonstrated in a recent work in which PSCs based on pure isomers of [70]fullerene monoadducts, separated all of them by HPLC,

[a] Dr. S. Vidal, Dr. M. Izquierdo, Dr. S. Filippone, Dr. I. Fernández, Prof. N. Martín
Department of Organic Chemistry, University Complutense
Avenida Complutense s/n; 28040 Madrid (Spain)
E-mail: nazmar@ucm.es

[b] S. Akin, Dr. J.-Y. Seo, Dr. S. M. Zakeeruddin, Prof. M. Grätzel
Laboratory of Photonics and Interfaces
Institute of Chemical Sciences and Engineering
École Polytechnique Fédérale de Lausanne (EPFL)
Station 6, 1015, Lausanne (Switzerland)
E-mail: shaik.zakeer@epfl.ch
michael.graetzel@epfl.ch

[c] S. Akin
Department of Metallurgical and Materials Engineering
Karamanoglu Mehmetbey University, 70100, Karaman (Turkey)

[d] Prof. N. Martín
IMDEA-Nanociencia, C/Faraday, 9
Campus de Cantoblanco, 28049 Madrid (Spain)

Supporting information and the ORCID identification number(s) for the author(s) of this article can be found under: https://doi.org/10.1002/chem.201806053.

achieved greater efficiencies than the devices based on the mixture of isomers.[13] Furthermore, a slightly beneficial performance has been found for α-pure [70]PCBM site-isomer devices when compared with commercially available α+β isomeric mixture in organic photovoltaic devices.[6a, 12d] Despite the interest in isomerically pure samples of [70]fullerene derivatives, these are obtained by tedious and time-consuming HPLC techniques.[6]

In this work, we report an alternative and highly efficient methodology based on mild conditions to obtain [70]methanofullerenes PCBM-like derivatives that allows us to direct the site-selectivity of the cycloaddition to the alpha or to the beta isomer, depending on the solvent polarity. This approach enables to obtain substantial amounts of both α and β site-isomers. This new set of pure [70]fullerene derivatives was applied as interface passivation materials in PSCs in order to determine the isomer effect on the photovoltaic properties.

Cyclopropanation is one of the most common chemical modifications in fullerenes chemistry due to the robustness and the easy preparation of the resulting methanofullerenes.[14] Among the different synthetic approaches to obtain methanofullerenes, the reaction of stabilized sulfur ylides derived from halocarbonyl compounds, leads only to [6,6]-closed methanofullerenes.[15] This methodology was selected for the synthesis of new fullerene derivatives with a high isomeric purity. In particular, we have used the α-bromo-derivative **1** whose structure resembles that contained in the well-known PCBM molecule.

α-Bromo-acetophenyl methyl ester **1** reacted with dimethylsulfide and silver tetrafluoroborate to afford the sulfonium salt **2**. To a solution of C_{70} and **2** in *o*-DCB was added triethylamine, and the reaction mixture was stirred at room temperature for 2 hours affording exclusively the expected α-site isomer **3** in 70% yield (based on recovered C_{70}) (Scheme 1). The selectivity of this reaction was determined by HPLC analysis and NMR spectroscopy (see Supporting Information).

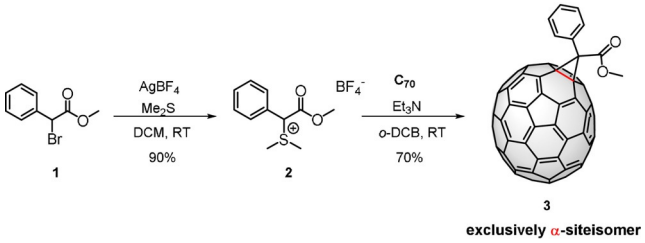

Scheme 1. Selective synthesis of α-site-isomer **3** from a sulfonium salt.

Compound **3** was isolated by silica-gel column chromatography and characterized by standard spectroscopic techniques (see the Supporting Information).

It is well-known that in α-bonds the curvature strain is higher than that of β-double bonds. Therefore, the α-bond in [70]fullerene is the most reactive and, as a consequence, the β-site isomers are typically obtained as minor products in significantly lower yields. For this reason, the reactivity and electrochemical properties of these isomers have been barely studied.

Thus, we first focused our attention on developing an alternative [70]methanofullerene synthesis by switching the site selectivity toward the less reactive β-double bond. Under standard Bingel cyclopropanation conditions, a solution of [70]fullerene and α-Br-acetophenyl methyl ester **1** in the presence of a base, gives rise to a mixture of α- and β-site-isomers in a **75:25** ratio. In sharp contrast, if the reaction is carried out in a polar solvent (DMF) the ratio α:β is significantly inverted to **32:68** (Scheme 2).

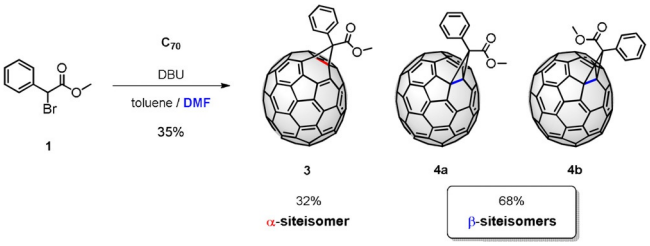

Scheme 2. Synthesis of enriched β-site isomers **4a,b**.

To the best of our knowledge, this is the first time that a β-site isomer is obtained as the main product of an addition reaction on [70]fullerene. This experimental finding paves the way to investigate a new reactivity on C_{70} and to explore the properties of these less-known β-derivatives.

Cyclic voltammetry of α-site-isomer **3** and β-site-isomers **4a,b** was carried out in *o*-DCB/ACN 4:1 using a GCE (glassy carbon electrode) as the working electrode, $Ag/AgNO_3$ as the reference electrode and $Bu_4N{\cdot}PF_6$ as the supporting electrolyte. The first reversible reduction potentials of **3** (−1.10 V) and **4a,b** (−1.07 V) reveal that these compounds are slightly better electron acceptors (around 20–30 mV) than the corresponding [70]PCBM site-isomers. These data could be accounted for by the direct binding of the electron-withdrawing ester group to the bridgehead carbon of [70]methanofullerenes (see Supporting Information).

Density functional theory (DFT) calculations were carried out at the PCM(DMF)-B3LYP-D3/def2-TZVPP//PCM(DMF)-B3LYP-D3/def2-SVP level[16] to gain more insight into the site-selectivity of the above transformation. To this end, the reaction between C_{70} and the carbanion derived for **1** (readily formed upon reaction of **1** with the BDU base) was explored. As previously described for related Bingel reactions,[17] the transformation proceeds via an initial barrierless addition of the carbanion to the C_{70} followed by a S_N2-type reaction which affords the corresponding cyclopropane adduct releasing the bromide anion. As shown in Figure 1, although the formation of the α-adduct is, as expected, thermodynamically favored, the corresponding initial intermediate **INT1** as well as the transition state (**TS**) associated with the S_N2 reaction are favored for the β-pathway. Therefore, it can be assumed that the selectivity of the process is determined by the energy difference of the respective transition states. Indeed, the computed $\Delta\Delta G^{\neq}$(**α-TS-β-TS**) = 0.35 kcal mol^{-1} (at 298 K) is translated into a α:β ratio of 36:64, which is fully consistent with the experimentally observed ratio of 32:68.

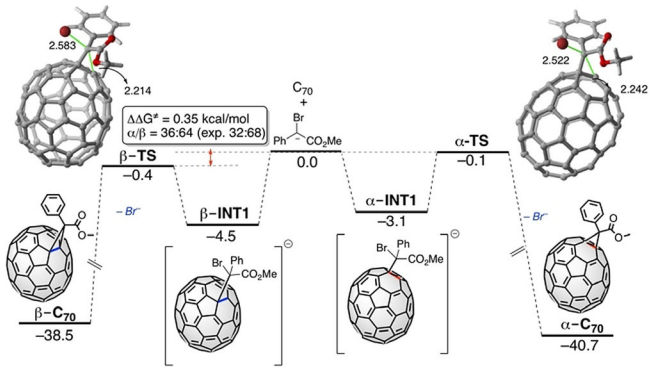

Figure 1. Computed reaction profile for the reaction between C_{70} and **1**(−). Relative free energies (ΔG, at 298 K) and bond distances are given in kcal mol^{-1} and angstroms, respectively. All data have been computed at the PCM(DMF)-B3LYP-D3/def2-TZVPP//PCM(DMF)-B3LYP-D3/def2-SVP level.

We repeated these calculations by replacing the DMF solvent by toluene. In these conditions, the corresponding transition states for both pathways are nearly degenerate ($\Delta\Delta G^{\neq}$(**α-TS-β-TS**) ≈ 0.0 kcal mol^{-1}), which although does not perfectly match the experimental ratio, is consistent with the observed influence of the polarity of the solvent on the site-selectivity of the transformation.

Bare chlorobenzene (CB, anti-solvent) and 0.4 mg mL^{-1} of PCBM-like derivatives (**3, 4** and **3** + **4** in a 32:68 ratio) containing CB anti-solvents were prepared to investigate the effect of the use, as templating agent, of these PCBM-like derivatives and their composition on the photovoltaic performance of devices.

The impact of anti-solvent treatment on the surface morphology of perovskite films was investigated by FE-SEM images (see Figure S10a–f). As clearly seen in the top-view FE-SEM image of perovskite film treated with only CB (Figure S10a), several pin-holes (marked with red circles) located at grain boundaries can be observed. Owing to this poor and highly rough morphology, the undesirable direct contacts (shunt paths) between the HTM and TiO_2 will exist and charge recombination will increase accordingly.[18] Furthermore, deep slits (marked with yellow rectangular) extending along the grain boundaries promote critical current leakages due to the lack of inter-connection between grains.[19] As a result, a remarkable degradation in the overall device performance will be inevitable. On the other hand, the density of pin-holes and/or deep slits along the grain boundaries was significantly prevented for α-site isomer **3** and β-site isomer **4** containing perovskite surfaces whereas anti-solvent treatment with **3** + **4** presented a pin-hole free and smoother perovskite formation. The effect of PCBM-like derivatives-containing anti-solvent treatment can be ascribed to being occupied of vacancies/pin-holes by PCBM molecules, indicating a compact/dense and highly smooth perovskite surface.[20] The enhancement of surface morphology was further supported by the contact angle measurements between corresponding perovskite films and water molecules (inset of Figure S10a–d). The only CB containing perovskite film exhibited a 48°, while, **3**, **4**, and **3** + **4** anti-solvents treated perovskite films exposed a prevailing hydrophobicity of 63–65°, leading to a long-term tolerance humidity of the device by prohibiting the water ingression into the perovskite film.[21–22] The cross-sectional FE-SEM images of devices with only CB (Figure S10e) and **3** + **4** (Figure S10f) anti-solvent treated perovskite layers indicated not only well defined/interconnected interfaces but also similar perovskite thickness (ca. 500 nm).

It is clear that perovskite films processed with PCBM derivatives-containing anti-solvent treatment have similar absorption profiles, with a strong absorption ranging from 450 to 800 nm (Figure S10g). A comparable absorption between 600 and 800 nm was observed, but the absorption intensity of only CB treated perovskite film is relatively lower in the range of 450–600 nm. This difference leading to a better light harvesting efficiency may be originated from highly smooth and/or fully covered compact surface.[22] All the perovskite films possess a similar absorption edge (≈785 nm) and the optical band gap almost remains the same (≈1.58 eV) for various anti-solvent treatments. This result was further confirmed by steady-state PL measurements of the perovskite films. As can be seen in Figure S10h, there is no obvious shift in the peak position of perovskite films. On the other hand, the highest PL intensity was observed for only CB treated perovskite film while the lowest one observed for **3** + **4** anti-solvent-treated perovskite. The reduced PL intensity can be ascribed to better charge injection into the ETL, which is promising for higher J_{sc}.[23] Furthermore, a slight blue-shifting and narrowing for PCBM-derivatives anti-solvent treated perovskite films can be clearly seen in normalized steady-state PL spectra of corresponding films compared to only CB treated one (inset of Figure S10h). These changes (quenching, blueshifting, and narrowing) in PL peaks of PCBM-derivatives can be attributed to the decrease of recombination center's density between trap states in perovskite structure, indicating a fast charge collecting efficiency.[23] Therefore, the incorporation of PCBM-derivatives as dopants into CB anti-solvent was highly encouraging in the PSCs in terms of void-free and dense morphology, indicating a superior charge transportation.[10d,22] Figure S10i shows time-resolved PL (TR-PL) decay measurements. The PL decay curves were fitted as reported in our previous work.[24] The α-site isomer, β-site isomer, and α + β-mixture containing perovskite films, respectively showed average lifetimes of (τ_{av}) 229, 259, and 321 ns while only CB treated control film gave 174 ns. A long decay time indicates a long exciton diffusion length and low defect concentration in the perovskite structure, hence better electronic quality for all PCBM-containing perovskite film. This is a promising preliminary result for obtaining high V_{oc} values of the corresponding devices.[22,23] After the examination of PCBM-derivatives treatments on perovskite films, PSCs were prepared to investigate the effect of current approach on the overall photovoltaic performance. Table 1 shows the output characteristics of the all devices. As compared to only CB (19.1 ± 0.1) treated control device, α-site isomer **3** (19.8 ± 0.3), β-site isomer **4** (19.7 ± 0.1), and α + β-mixture of **3** + **4** (20.3 ± 0.2) treatments showed a remarkable improvement in the photovoltaic parameters, which resulted in an average power conversion efficiency (PCE) increment for devices. The highest PCE value of 20.5%

Table 1. Best and average photovoltaic performances of only CB and PCBM-derivatives treated PSCs.

Device[a]	V_{oc} (V) Best (average)	J_{sc} (mA cm^{-2}) Best (average)	FF Best (average)	PCE (%) Best (average)
Only CB	1.08 (1.06 ± 0.01)	23.7 (23.4 ± 0.2)	0.75 (0.75 ± 0.01)	19.3 (19.1 ± 0.1)
3	1.11 (1.09 ± 0.01)	23.9 (23.7 ± 0.2)	0.76 (0.76 ± 0.02)	20.1 (19.8 ± 0.3)
4	1.09 (1.08 ± 0.01)	23.9 (23.8 ± 0.2)	0.77 (0.76 ± 0.01)	19.8 (19.7 ± 0.1)
3 + **4**	1.10 (1.09 ± 0.01)	24.0 (23.9 ± 0.1)	0.78 (0.77 ± 0.01)	20.5 (20.3 ± 0.2)

[a] 5 devices for **3** and **4** and 10 devices for control and **3** + **4**; The voltage scan rate for all scans was 10 mV s^{-1} and no device preconditioning, that is, light soaking or forward voltage bias applied for a long time, was applied before starting the measurement.

were achieved for α + β-mixture of **3** + **4** + CB treated perovskite devices, and their current density–voltage (*J*–*V*) curves under AM 1.5G irradiation of 100 mW cm^{-2} were depicted in Figure 2 along with the best performed cell treated only with CB.

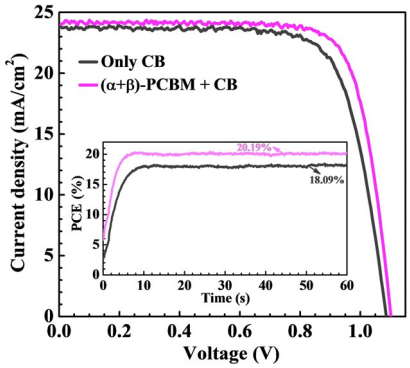

Figure 2. *J*–*V* and maximum power point (mpp) tracking (as the inset) curves of the champion cells based on only CB (black) and α + β-mixture of **3** + **4** + CB (purple) treated perovskites.

The integrated J_{sc} values and perceivable increase in EQE spectra (Figure S11a) are consistent with the J_{sc} values determined from *J*–*V* curves and absorption spectra, respectively. The stabilized power was monitored at maximum power point (mpp) as a function of time (inset of Figure 2), showing the resulting power output of 18.1 and 20.2 mW cm^{-2}, for only CB and **3** + **4** + CB treated PSCs, respectively. The difference in PCEs can be ascribed to the *J*–*V* hysteresis effect in the device. The scan direction measurements were then performed to evaluate the hysteresis behaviors of only CB and **3** + **4** + CB treated PSCs (Figure S11b). These results showed a similar tendency with the mpp outputs. The hysteresis in **3** + **4** + CB device is negligible, with a small PCE discrepancy between forward and reverse scans (≈0.3% absolute PCE), whereas the control device exhibits a considerable hysteresis in *J*–*V* scans (≈1.5% absolute PCE). The higher degree of hysteresis in only CB treated control device is mainly owing to higher density of traps in the perovskite film.[25] The best cell performance of **3** + **4** + CB treatment, among 10 devices, afford an open-circuit voltage (V_{oc}) of 1.10 V, a short-circuit current density (J_{sc}) of 24.0 mA cm^{-2} and a fill factor (FF) of 0.78. This enhancement can be ascribed to the compact and smooth surface morphology obtained by hindering of pin-holes and deep borders. This can help to inhibit undesirable current leakages and thus improve the photovoltaic performance, especially in terms of FF. Statistical results for the photovoltaic parameters with respect to the anti-solvent treatment can be found in Figure S12 (please see SI). The excellent reproducibility of **3** + **4** + CB treated PSCs with narrow statistical distribution of the photovoltaic metrics is tabulated in Table 1.

Finally, we assessed the long-term shelf stability of the non-encapsulated devices in the dark with a relative humidity of 40–60% (Figure S11c). After 30 days, the **3** + **4** anti-solvent treated PSC retained 80% of its initial efficiency, while the PCE of the control PSC dropped to 44%, as revealed by contact angle measurement. We can ascribe the improved stability of PCBM-derivatives containing PSC to less pin-holes and lack of obvious deep-slits, which minimizes the decomposition of the active layer via moisture, current leakage, and immigration of Li ions from spiro-OMETAD into perovskite and ETL.

In conclusion, we have selectively synthesized α and β site-isomers of [70]methanofullerenes PCBM-like derivatives and employed them as interface passivation materials in PSCs to determine the isomer effect on the photovoltaic properties. This facile approach positively addresses the issues of poor surface morphology of perovskites by passivating the voids/pin-holes and/or deep slits, resulting in a highly efficient and stable bulk heterojunction PSCs. Interestingly, these experimental findings pave the way to investigate a new reactivity on C_{70} and to explore the properties of the less-known [70]fullerene β-derivatives.

Experimental Section

Experimental details are included in the Supporting Information.

Acknowledgements

N.M.L. acknowledges support from the European Research Council (ERC-320441-Chirallcarbon), the MINECO of Spain (projects CTQ2017-83531-R and CTQ2016-81911-REDT) and the Comunidad de Madrid (PHOTOCARBON project S2013/MIT-2841), IMDEA Nanociencia thanks support from the "Severo Ochoa" Programme for Centers of Excellence in R&D (MINECO, Grant SEV-2016-0686); I.F. thanks the Spanish MINECO-FEDER (Grants CTQ2016-78205-P and CTQ2016-81797-REDC); M.I. thanks the

MINECO of Spain (JC IJCI-2014–19320). S.A. would like to thank TUBITAK-2214-A International Doctoral Research Fellowship Programme, for supporting his research at EPFL. S.M.Z. and M.G. thank the King Abdulaziz City for Science and Technology (KACST) for financial support.

Conflict of interest

The authors declare no conflict of interest.

Keywords: cyclopropanation reaction · fullerenes · interface passivation · perovskite solar cells · site-selectivity

[1] a) A. B. Sieval, J. C. Hummelen, in *Organic Photovoltaics*, Wiley-VCH, Weinheim, **2014**, pp. 209 – 238; b) B. C. Thompson, J. M. J. Frechet, *Angew. Chem. Int. Ed.* **2008**, *47*, 58 – 77; *Angew. Chem.* **2008**, *120*, 62 – 82; c) J. L. Delgado, S. Filippone, F. Giacalone, M. A. Herranz, B. Illescas, E. M. Pérez, N. Martín, *Top. Curr. Chem.* **2014**, *350*, 1 – 64.

[2] a) D. M. Guldi, N. Martín, *Fullerenes: From Synthesis to Optoelectronic Properties*, Springer Netherlands, **2002**; b) J. L. Delgado, P.-A. Bouit, S. Filippone, M. A. Herranz, N. Martín, *Chem. Commun.* **2010**, *46*, 4853 – 4865; c) G. Dennler, M. C. Scharber, C. J. Brabec, *Adv. Mater.* **2009**, *21*, 1323 – 1338; d) B. Kippelen, J.-L. Brédas, *Energy Environ. Sci.* **2009**, *2*, 251 – 261; e) N. Martín, *Adv. Energy Mater.* **2017**, *7*, 1601102; f) E. E. Maroto, M. Izquierdo, S. Reboredo, J. Marco-Martínez, S. Filippone, N. Martín, *Acc. Chem. Res.* **2014**, *47*, 2660 – 2670; g) S. Bosi, T. Da Ros, G. Spalluto, M. Prato, *Eur. J. Med. Chem.* **2003**, *38*, 913 – 923; h) D. M. Guldi, M. Prato, *Acc. Chem. Res.* **2000**, *33*, 695 – 703.

[3] a) D. M. Guldi, B. M. Illescas, C. M. Atienza, M. Wielopolski, N. Martín, *Chem. Soc. Rev.* **2009**, *38*, 1587 – 1597; b) D. Kronholm, J. C. Hummelen, *Material Matters* **2007**, *2*, 16 – 20.

[4] a) M. T. Rispens, A. Meetsma, R. Rittberger, C. J. Brabec, N. S. Sariciftci, J. C. Hummelen, *Chem. Commun.* **2003**, 2116 – 2118; b) S. Vela, S. Bauroth, C. Atienza, A. Molina-Ontoria, D. M. Guldi, N. Martín, *Angew. Chem. Int. Ed.* **2016**, *55*, 15076 – 15080; *Angew. Chem.* **2016**, *128*, 15300 – 15304; c) L. Sánchez, R. Otero, J. M. Gallego, R. Miranda, N. Martín, *Chem. Rev.* **2009**, *109*, 2081 – 2091.

[5] J. W. Arbogast, C. S. Foote, *J. Am. Chem. Soc.* **1991**, *113*, 8886 – 8889.

[6] a) S. Vidal, M. Izquierdo, W. K. Law, K. Jiang, S. Filippone, J. Perles, H. Yan, N. Martín, *Chem. Commun.* **2016**, *52*, 12733 – 12736; b) E. E. Maroto, A. de Cózar, S. Filippone, A. Martín-Domenech, M. Suarez, F. P. Cossío, N. Martín, *Angew. Chem. Int. Ed.* **2011**, *50*, 6060 – 6064; *Angew. Chem.* **2011**, *123*, 6184 – 6188. In this paper, some indications for the use of "site-isomers" nomenclature is given.

[7] a) C. L. Chochos, N. Tagmatarchis, V. G. Gregoriou, *RSC Adv.* **2013**, *3*, 7160 – 7181; b) Y.-J. Hwang, B. A. E. Courtright, A. S. Ferreira, S. H. Tolbert, S. A. Jenekhe, *Adv. Mater.* **2015**, *27*, 4578 – 4584; c) Y. Zhong, M. T. Trinh, R. Chen, G. E. Purdum, P. P. Khlyabich, M. Sezen, S. Oh, H. Zhu, B. Fowler, B. Zhang, W. Wang, C.-Y. Nam, M. Y. Sfeir, C. T. Black, M. L. Steigerwald, Y.-L. Loo, F. Ng, X. Y. Zhu, C. Nuckolls, *Nat. Commun.* **2015**, *6*, 8242; d) Y. Lin, T. Li, F. Zhao, L. Han, Z. Wang, Y. Wu, Q. He, J. Wang, L. Huo, Y. Sun, C. Wang, W. Ma, X. Zhan, *Adv. Energy Mater.* **2016**, *6*, 1501063; e) L. Gao, Z. G. Zhang, L. Xue, J. Min, J. Zhang, Z. Wei, Y. Li, *Adv. Mater.* **2016**, *28*, 1884 – 1890.

[8] A. Kojima, K. Teshima, Y. Shirai, T. Miyasaka, *J. Am. Chem. Soc.* **2009**, *131*, 6050 – 6051.

[9] https://www.nrel.gov/pv/assets/pdfs/pv-efficiencies-12-14-2018.pdf.

[10] a) L. Meng, J. You, T.-F. Guo, Y. Yang, *Acc. Chem. Res.* **2016**, *49*, 155 – 165; b) R. Sandoval-Torrientes, J. Pascual, I. García-Benito, S. Collavini, I. Kosta, R. Tena-Zaera, N. Martín, J. L. Delgado, *ChemSusChem* **2017**, *10*, 2023 – 2029; c) T. Gatti, E. Menna, M. Meneghetti, M. Maggini, A. Petrozza, F. Lamberti, *Nano Energy* **2017**, *41*, 84 – 100; d) F. Zhang, W. Shi, J. Luo, N. Pellet, C. Yi, X. Li, X. Zhao, T. J. S. Dennis, X. Li, S. Wang, Y. Xiao, S. M. Zakeeruddin, D. Bi, M. Grätzel, *Adv. Mater.* **2017**, *29*, 1606806; e) S. R. Peurifoy, E. Castro, F. Liu, X. Y. Zhu, F. Ng, S. Jockusch, M. L. Steigerwald, L. Echegoyen, C. Nuckolls, T. J. Sisto, *J. Am. Chem. Soc.* **2018**, *140*, 9341 – 9345.

[11] a) I. Zimmermann, J. Urieta-Mora, P. Gratia, J. Aragó, G. Grancini, A. Molina-Ontoria, E. Ortí, N. Martín, M. K. Nazeeruddin, *Adv. Energy Mater.* **2017**, *7*, 1601674; b) I. García-Benito, I. Zimmermann, J. Urieta-Mora, J. Aragó, A. Molina-Ontoria, E. Ortí, N. Martín, M. K. Nazeeruddin, *J. Mater. Chem. A* **2017**, *5*, 8317 – 8324; c) A. Molina-Ontoria, I. Zimmermann, I. Garcia-Benito, P. Gratia, C. Roldán-Carmona, S. Aghazada, M. Graetzel, M. K. Nazeeruddin, N. Martín, *Angew. Chem. Int. Ed.* **2016**, *55*, 6270 – 6274; *Angew. Chem.* **2016**, *128*, 6378 – 6382; d) L. Calió, S. Kazim, M. Grätzel, S. Ahmad, *Angew. Chem. Int. Ed.* **2016**, *55*, 14522 – 14545; *Angew. Chem.* **2016**, *128*, 14740 – 14764; e) N. J. Jeon, H. Na, E. H. Jung, T.-Y. Yang, Y. G. Lee, G. Kim, H.-W. Shin, S. Il Seok, J. Lee, J. Seo, *Nat. Energy* **2018**, *3*, 682 – 689; f) I. García-Benito, I. Zimmermann, J. Urieta-Mora, J. Aragó, J. Calbo, J. Perles, A. Serrano, A. Molina-Ontoria, E. Ortí, N. Martín, M. K. Nazeeruddin, *Adv. Funct. Mater.* **2018**, *28*, 1801734; g) J. Urieta-Mora, I. García-Benito, A. Molina-Ontoria, N. Martín, *Chem. Soc. Rev.* **2018**, *47*, 8541 – 8571.

[12] a) S. Kitaura, K. Kurotobi, M. Sato, Y. Takano, T. Umeyama, H. Imahori, *Chem. Commun.* **2012**, *48*, 8550 – 8552; b) Y. Liu, J. Zhao, Z. Li, C. Mu, W. Ma, H. Hu, K. Jiang, H. Lin, H. Ade, H. Yan, *Nat. Commun.* **2014**, *5*, 5293; c) X. Meng, G. Zhao, Q. Xu, Z. A. Tan, Z. Zhang, L. Jiang, C. Shu, C. Wang, Y. Li, *Adv. Funct. Mater.* **2014**, *24*, 158 – 163; d) T. Umeyama, T. Miyata, A. C. Jakowetz, S. Shibata, K. Kurotobi, T. Higashino, T. Koganezawa, M. Tsujimoto, S. Gélinas, W. Matsuda, S. Seki, R. H. Friend, H. Imahori, *Chem. Sci.* **2017**, *8*, 181 – 188; e) S.-M. Dai, X. Zhang, W.-Y. Chen, X. Li, Z. A. Tan, C. Li, L.-L. Deng, X.-X. Zhan, M.-S. Lin, Z. Xing, T. Wen, R.-M. Ho, S.-Y. Xie, R.-B. Huang, L.-S. Zheng, *J. Mater. Chem. A* **2016**, *4*, 18776 – 18782.

[13] E. Castro, G. Zavala, S. Seetharaman, F. D'Souza, L. Echegoyen, *J. Mater. Chem. A* **2017**, *5*, 19485 – 19490.

[14] M. Yamada, T. Akasaka, S. Nagase, *Chem. Rev.* **2013**, *113*, 7209 – 7264.

[15] a) T. Tada, Y. Ishida, K. Saigo, *J. Org. Chem.* **2006**, *71*, 1633 – 1639; b) T. Ito, T. Iwai, F. Matsumoto, K. Hida, K. Moriwaki, Y. Takao, T. Mizuno, T. Ohno, *Synlett* **2013**, *24*, 1988 – 1992.

[16] See Computational Details in the Supporting Information.

[17] a) M. Garcia-Borràs, M. R. Cerón, S. Osuna, M. Izquierdo, J. M. Luis, L. Echegoyen, M. Solà, *Angew. Chem. Int. Ed.* **2016**, *55*, 2374 – 2377; *Angew. Chem.* **2016**, *128*, 2420 – 2423; b) N. M. Thong, T. C. Ngo, D. Q. Dao, T. Duong, Q. T. Tran, P. C. Nam, *J. Mol. Model.* **2016**, *22*, 113.

[18] S. Paek, P. Schouwink, E. N. Athanasopoulou, K. T. Cho, G. Grancini, Y. Lee, Y. Zhang, F. Stellacci, M. K. Nazeeruddin, P. Gao, *Chem. Mater.* **2017**, *29*, 3490 – 3498.

[19] I. Zarazúa, S. Sidhik, T. Lopez-Luke, D. Esparza, E. De la Rosa, J. Reyes-Gómez, I. Mora-Sero, G. García-Belmonte, *J. Phys. Chem. Lett.* **2017**, *8*, 6073 – 6079.

[20] S. Yoon, M. W. Ha, D. W. Kang, *J. Mater. Chem. C* **2017**, *5*, 10143 – 10151.

[21] J. Y. Seo, H. S. Kim, S. Akin, M. Stojanovic, E. Simon, M. Fleischer, A. Hagfeldt, S. M. Zakeeruddin, M. Grätzel, *Energy Environ. Sci.* **2018**, *11*, 2985 – 2992.

[22] a) S. Akin, Y. Liu, M. I. Dar, S. M. Zakeeruddin, M. Gratzel, S. Turan, S. Sonmezoglu, *J. Mater. Chem. A* **2018**, *6*, 20327 – 20337; b) H. Zhu, F. Zhang, Y. Xiao, S. Wang, X. Li, *J. Mater. Chem. A* **2018**, *6*, 4971 – 4980.

[23] a) K. Wang, C. Liu, P. C. Du, J. Zheng, X. Gong, *Energy Environ. Sci.* **2015**, *8*, 1245 – 1255; b) Q. F. Dong, Y. J. Fang, Y. C. Shao, P. Mulligan, J. Qiu, L. Cao, J. S. Huang, *Science* **2015**, *347*, 967 – 970.

[24] D. Bi, X. Li, J. V. Milić, D. J. Kubicki, N. Pellet, J. Luo, T. L. Grange, P. Mettraux, L. Emsley, S. M. Zakeeruddin, M. Grätzel, *Nat. Commun.* **2018**, *9*, 4482 – 4491.

[25] a) H. R. Tan, A. Jain, O. Voznyy, X. Z. Lan, F. P. G. de Arquer, J. Z. Fan, R. Quintero-Bermudez, M. J. Yuan, B. Zhang, Y. C. Zhao, F. J. Fan, P. C. Li, L. N. Quan, Y. B. Zhao, Z. H. Lu, Z. Y. Yang, S. Hoogland, E. H. Sargent, *Science* **2017**, *355*, 722 – 726; b) Y. Shao, Z. Xiao, C. Bi, Y. Yuan, J. Huang, *Nat. Commun.* **2014**, *5*, 5784 – 5787.

Manuscript received: December 5, 2018
Revised manuscript received: January 9, 2019
Version of record online: January 29, 2019